

ARTICLES

Influence of Calcining Temperature on Photoluminescence and Triboluminescence of Europium-Doped Strontium Aluminate Particles Prepared by Sol–Gel Process

Yun Liu[†] and Chao-Nan Xu^{*,†,‡}

National Institute of Advanced Industrial Science and Technology (AIST), Shuku, 807-1, Tosu, Saga, 841-0052, Japan, and PRESTO, Japan Science and Technology Corporation (JST), Honcho 4, Kawaguchi, Saitama 332-0012, Japan

Received: September 13, 2002; In Final Form: December 1, 2002

On the basis of a new modified base-catalyzed sol–gel process and a careful investigation in the structure, this study systematically discussed the effects of the calcining temperature on the microstructure and luminescent properties of europium-doped strontium aluminates (SAO-E). A phase transformation from $\text{Sr}_3\text{Al}_2\text{O}_6$ to SrAl_2O_4 is found with increasing calcining temperature. The SAO-E sample calcined at 1400 °C for 2 h possesses a SrAl_2O_4 single monoclinic phase (space group $P2_1$). The light emission transition of SAO-E particles at low calcining temperature originated from both Eu^{2+} and Eu^{3+} ions where the trivalent europium ions were proved to be incorporated in the SrAl_2O_4 phase, which gradually transformed into the divalent ions with increasing calcining temperature. The strong photoluminescence and triboluminescence were obtained without luminance temperature-degradation in this single monoclinic SrAl_2O_4 phase.

Introduction

The europium-doped strontium aluminates (SAO-E) have been well-known as a green phosphor. Their no radiation and bright luminescence have attracted great interest for applications in the lamp, the cathode-ray tube (CRT), and the plasma display panel (PDP).^{1–5} Recently, we also discovered a strong mechanoluminescent property in $\text{Eu}:\text{SrAl}_2\text{O}_4$, which can be utilized in the visualization of stress distribution and other mechano-optical devices.^{6–9} Several attempts to prepare this kind of material have been carried out in this decade. The traditional process was based on the solid-state reaction, which often needed a high calcining temperature up to 1600 °C, or some additives as flux, to get a single phase. Ito et al.¹⁰ reported the

synthesis of the SAO-E particles with an “alleged α -type” monoclinic structure, where the lattice constants are $a = 10.20$ Å, $b = 20.26$ Å, and $c = 8.42$ Å, $\gamma = 119.47^\circ$. However, no further work proved its reality. The $\text{Eu}:\text{SrAl}_2\text{O}_4$ particles reported in Murayama’s patent¹¹ also contained the impure peaks in the XRD pattern in addition to the SrAl_2O_4 phase. Tang¹² proclaimed that they obtained the nanometer SAO-E powders, but their XRD pattern was composed of impure phase together with the SrAl_2O_4 phase. It seems extremely difficult to control the formation of the single phase of $\text{Eu}:\text{SrAl}_2\text{O}_4$ with fine particles. On the other hand, Song and co-workers¹³ have just studied the emission spectra of $\text{Sr}_3\text{Al}_2\text{O}_6/\text{SrAl}_2\text{O}_4$ mixing phases, which indicated that the existence of the impure phase in $\text{Eu}:\text{SrAl}_2\text{O}_4$ greatly affected its luminescent property. In consideration of this case, a new modified base-catalyzed sol–gel process was proposed in this study, which makes it possible for getting a pure SrAl_2O_4 phase. Further, it becomes possible to factually reveal the relationship between the phase structure

* Author to whom correspondence should be addressed. E-mail: cn-xu@aist.go.jp.

[†] National Institute of Advanced Industrial Science and Technology (AIST).

[‡] PRESTO, Japan Science and Technology Corporation (JST).

and luminescence. We believe this work will greatly promote the development and application of the SAO-E phosphors with a high quality.

Experimental Section

Strontium aluminate powders were synthesized using a modified base-catalyzed sol-gel process. The initial composition was $\text{Sr}_{0.99}\text{Eu}_{0.01}\text{Al}_2\text{O}_4$. Amounts of 163.40 g of aluminum tri-isopropoxide ($\text{Al}(\text{O}-i\text{-C}_3\text{H}_7)_3$), 84.64 g of $\text{Sr}(\text{NO}_3)_3$, and 1.56 g of $\text{Eu}(\text{NO}_3)_3 \cdot 2.9\text{H}_2\text{O}$ were dissolved in 400 mL of ammonia water with a concentration of 0.5 M. $\text{Al}(\text{O}-i\text{-C}_3\text{H}_7)_3$ slowly hydrolyzed at 40 °C under the action of the base-catalysis and formed the $\text{Al}(\text{OR})_{3-x}(\text{OH})_x$ ($\text{R} = i\text{-C}_3\text{H}_7$). The condensation reaction led to the formation of polymeric local structure within the sol particles with a $\text{Sr}(\text{Eu})\text{-O-Al}$ bond. Subsequently, 200 mL of *N,N*-dimethylformamide (DMF) as the additive was added into the sol solution to coat the sol particles, to vary its surface activity, and to effectively control the growth of particles. The resultant sol solution was heated at 148 °C and then dried at 200 °C before completely gelling to obtain homogeneous smaller gel particles with an organic-coating. These dry gel particles were heat-treated at 700 °C to remove the organic and inorganic groups in air atmosphere, followed by calcining at high temperature from 750 °C to 1400 °C for 2 h in a reducing atmosphere of 5% $\text{H}_2\text{-N}_2$ to crystallize and form the luminescent centers. The size of particles prepared using this process was approximately 1–2 μm on the basis of the SEM observation.

The microstructure of SAO-E particles was determined by an X-ray diffraction (XRD) technique. The photoluminescent property was characterized by a spectrofluorometer (FP-6500, Jasco) with an optical fiber system capable of the measurement in the range of 80–800 K. To easily evaluate triboluminescent (TrL) properties, each sample of 1.5 g was mixed with an optical epoxy resin of 6 g to produce a composite disk of 25 mm in diameter. The TrL intensity was measured by a photon counting system, which consists of a photomultiplier tube (R464S, Hamamatsu Photonics) and a photo counter (C5410-51, Hamamatsu Photonics) controlled by a computer.¹⁸

Results and Discussion

Figure 1 gives the XRD patterns of the SAO-E particles obtained at different calcining temperatures from 750 °C to 1400 °C for 2 h. It was found that the XRD patterns of the SAO-E particles calcined at 750 °C consisted of two phases, the $\text{Sr}_3\text{Al}_2\text{O}_6$ and SrAl_2O_4 . The phase composition of the SrAl_2O_4 and $\text{Sr}_3\text{Al}_2\text{O}_6$ was evaluated as the ratio of the $P_{124}/(P_{124} + P_{326})$, which was about 53% at 750 °C as shown in Figure 2. This ratio reached 92% at 1000 °C and 97% at 1300 °C, respectively. It can be clearly seen that the $\text{Sr}_3\text{Al}_2\text{O}_6$ phase gradually transformed into the SrAl_2O_4 phase as the calcining temperature rises, and finally disappeared at a calcining temperature of 1400 °C. The single SrAl_2O_4 phase was consequently formed at a calcining temperature of 1400 °C for 2 h, which belongs to the monoclinic phase (space group $P2_1$) with $a = 5.163 \text{ \AA}$, $b = 8.447 \text{ \AA}$, $c = 8.816 \text{ \AA}$, and $\beta = 93.42^\circ$. We did not observe the so-called “alleged α -type” monoclinic structure.¹⁰

Figure 3 shows the excitation spectra of the SAO-E particles at different calcination temperatures under an emission of 519 nm. A significant difference was observed in the profile of the excitation spectra: the single excitation peak was found in the SAO-E particles at 365 nm at 750 °C and 1000 °C, but the double peaks were marked at 374 nm and 395 nm for 1300 °C and 1400 °C. The peak intensity at a wavelength of 395 nm increased

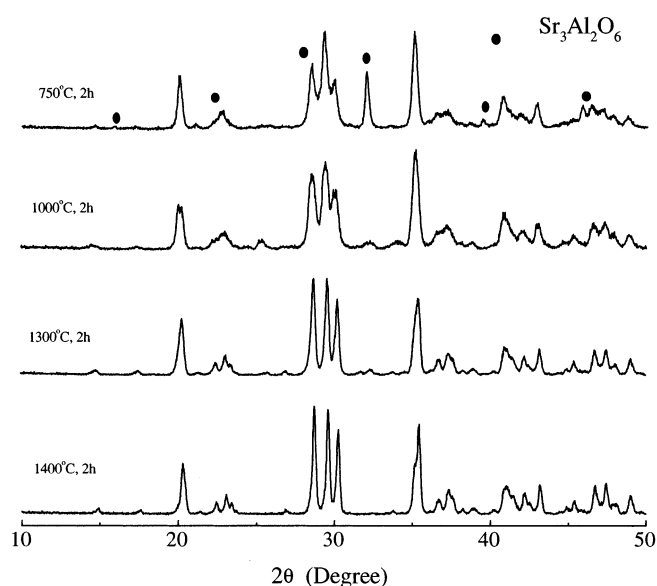


Figure 1. XRD patterns of the SAO-E particles calcined at different temperatures.

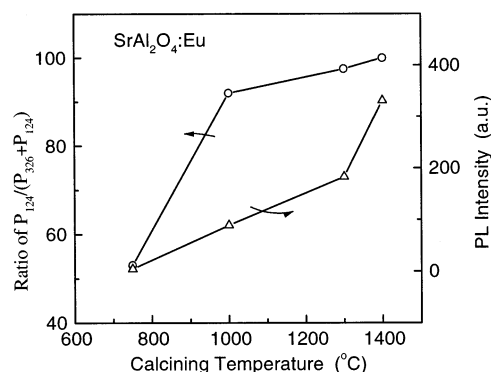


Figure 2. Influence of calcining temperature on phase composition and PL intensity.

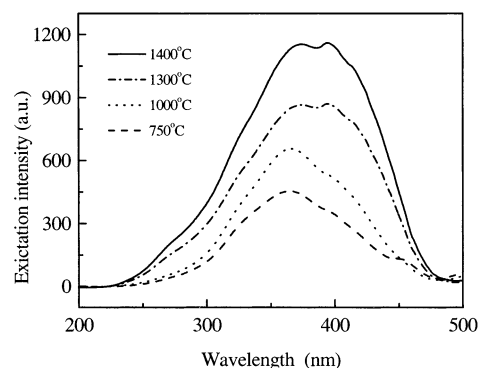


Figure 3. Excitation spectra of the SAO-E particles at different temperatures under an emission of 519 nm.

with the increasing of the calcination temperature. The single phase SrAl_2O_4 particles possessed a wide excitation spectrum and strong excitation intensity, in comparison with the SAO-E particles composing of two phases ($\text{Sr}_3\text{Al}_2\text{O}_6$ and SrAl_2O_4). This is possibly due to the variation in the splitting 5d levels caused by the deformation of the crystal field strength of the host. The d-orbital is generally a 5-fold degenerate in free space and it may further split under the action of the crystal field and the split interval should be proportional to the crystal field strength.

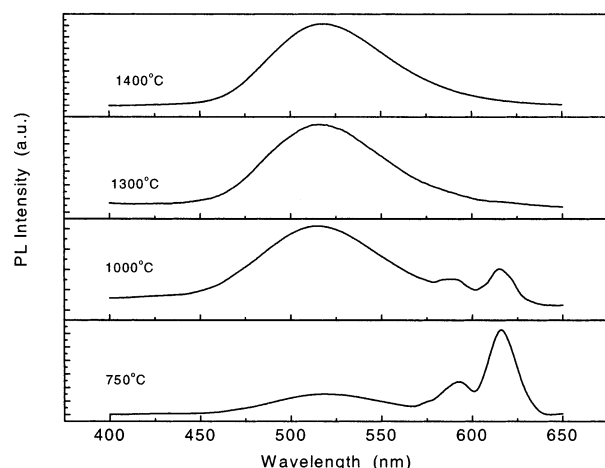


Figure 4. Emission spectra of the SAO-E particles at different temperatures under an excitation of 254 nm.

Accordingly, the different phase composition can lead to a change in the crystal field of the Eu^{2+} ion, and thus create different light absorption and excitation spectra. As we have known, the emission transition was considered to be the $\text{Eu}^{2+} 4f^65d \rightarrow 4f^7$ with a broad-featured spectrum in the visible light range, when the host material has a stronger crystal field strength.¹⁴ In SrAl_2O_4 , the $5d$ levels of the Eu^{2+} ions are located below the 6P_J state of the $4f^7$ configuration due to the strong crystal field strength, thus creating a broadband luminescence owing to the allowed $4f^65d \rightarrow 4f^7$ transition.

Emission spectra of the SAO-E particles at various calcining temperatures were also investigated under the excitation of different wavelengths in the range of 254–452 nm. The SAO-E particles calcined at 1400 °C had only one emission peak centered at 519 nm under the excitation of various wavelengths, as a result of the $5d \rightarrow 4f$ transition of Eu^{2+} ions in SrAl_2O_4 . Figure 4 shows the emission spectra of SAO-E particles calcined at various temperatures under the excitation of 254 nm. Contrary to SAO-E calcined at 1400 °C, the SAO-E particles calcined at 750 °C showed a red light emission within the range of 570–640 nm along with emission peak at 519 nm under the excitation of 254 nm. This red emission has a line-like feature, belonging to the emission from $\text{Eu}^{3+} {}^5D_0 \rightarrow {}^7F_J$ transitions, that is, there were trivalent europium ions in the SAO-E particles calcined at 750 °C. This red light emission decreased with the increasing calcining temperature and entirely disappeared at 1300 °C. In the emission spectra of the Eu^{3+} ions for the SAO-E sample calcined at 750 °C, the ${}^5D_0 \rightarrow {}^7F_2$ emission transition was prominent within the ${}^5D_0 \rightarrow {}^7F_J$ emission transition. In terms of the site-selected principle of the Eu^{3+} ion,¹⁵ in this study, the host should lack inversion symmetries, favoring the forced electric dipole transition in Eu^{3+} ions. The SrAl_2O_4 belongs to space group $P2_1$ without the inversion symmetry, but the $\text{Sr}_3\text{Al}_2\text{O}_6$ belongs to space group $Pa\bar{3}$ with a symmetrical center. It is therefore deduced that Eu^{3+} should appear in the SrAl_2O_4 phase. This point of view was not in agreement with the Song study.¹³ The Eu^{3+} and Eu^{2+} ions coexist in the SrAl_2O_4 particles, and create the trap centers such as Eu^{1+} and \square_{Sr} to maintain the balance of the valence. These trap centers were nonirradiation centers, which would greatly decrease the emission intensity of Eu^{2+} ions as shown in Figure 2.

From Figures 2 and 4, we also observe that the emission intensity at 519 nm significantly increased with the increasing calcining temperature. This was attributed to the phase transformation from $\text{Sr}_3\text{Al}_2\text{O}_6$ to SrAl_2O_4 . Generally, the emission level of Eu^{2+} ion is the $4f^65d^1$ configuration and the $5d$ electron

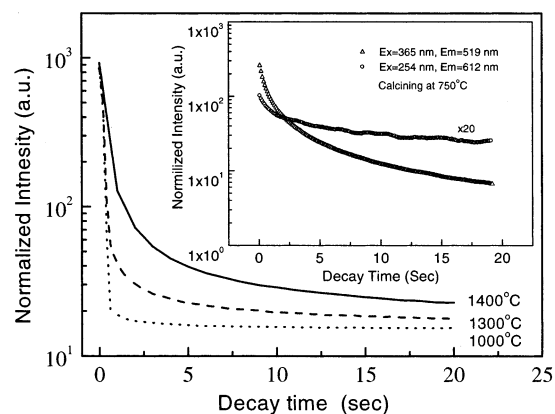


Figure 5. Decay curves of the afterglow of the SAO-E particles at different temperatures.

may couple strongly to the lattice; therefore, the energy level of $4f^65d^1$ would be strongly influenced by the crystal field strength. The $\text{Sr}_3\text{Al}_2\text{O}_6$ phase greatly varied the crystal field dependence of the $4f^65d^1$ energy level in the Eu^{2+} ion, and thus led to the variation in the excitation spectra and emission intensity. As a consequence, it can be concluded that the appearance of the $\text{Sr}_3\text{Al}_2\text{O}_6$ phase did not favor the light emission derived from the Eu^{2+} ions in SAO-E particles. The $\text{Sr}_3\text{Al}_2\text{O}_6$ phase content should be precisely controlled for high emission intensity.

Figure 5 shows the decay curves of the afterglow from the SAO-E particles calcined at different calcining temperatures. We did not find strong afterglow in all samples, because no trivalent hole trap centers, such as Dy^{3+} ions, existed in this material. It is in agreement with previous $\text{Eu}:\text{SrAl}_2\text{O}_4$ results where the particles were synthesized by a solid-state reaction.^{1,19} The SAO-E particles calcined at 750 °C showed 4% afterglow intensity as seen in the insert in Figure 5. It was also seen that the long decay intensity excited at a wavelength of 254 nm was much weaker than that at 365 nm for the sample calcined at 750 °C. This could be reasonably explained by the coexistence of the Eu^{3+} and Eu^{2+} ions in the SrAl_2O_4 on the basis of our above discussion. This phenomenon is similar to that of the Eu^{2+} and Dy^{3+} ions doubly doped SrAl_2O_4 where the long-persistent phosphorescence at room temperature is attributed to the electron-transfer process from Eu^{2+} to Dy^{3+} ions through the valance band.^{16,17,19} In our case, the Eu^{2+} ion is an emitter and the Eu^{3+} ion serves as a trapping center. In the samples calcined at temperatures from 1000 °C to 1400 °C, the decay time slightly increased as the calcining temperature rises. However, all the afterglow emission intensities were lower than 2.3%.

The thermoluminescence of the SAO-E particles calcined at different temperatures was also investigated in the temperature range of -50 °C to 250 °C. Before this measurement, the sample was first excited by UV at 365 nm for 5 min at -50 °C, then kept in dark for 30 min. Thermoluminescence glow curves were measured at different rates of heating. Figure 6 shows the thermoluminescence of various SAO-E particles at a heating rate of 3 °C/min. For the SAO-E particles calcined at 750 °C and 1000 °C, the defects were found to form a continual trap energy level. This was in agreement with the above discussion. The coexisting Eu^{3+} ions decreased the efficient emission centers from the Eu^{2+} ions and drop down the emission intensity at 519 nm. This continual trap level was separated into the two-overlapped trap energy levels at 1300 °C. For the SAO-E particles calcined at 1400 °C, two trap energy levels were further split and became two incoherent trap energy levels. The depth

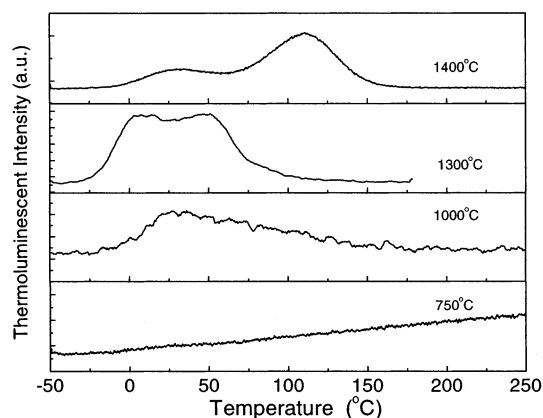


Figure 6. Thermoluminescence of the SAO-E particles at different temperatures.

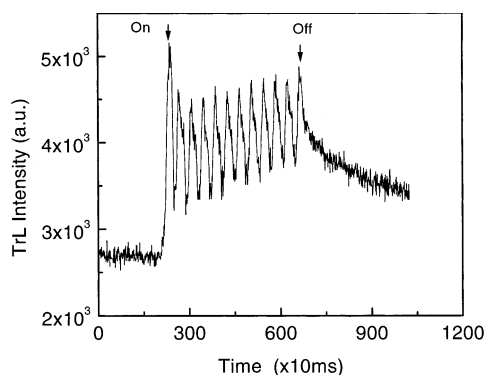


Figure 7. A typical triboluminescent response from an SAO-E composite.

of trap (E_t) was calculated from the slope of the Hoogenstraaten plots from the following equation:

$$E_t = -k \lg (\beta/T_m^2)/(1/T_m)$$

where k is the Boltzmann constant, β is the heating rate, and T_m represents the glow peak temperature. The two trap levels were then evaluated to be 0.34 eV and 0.80 eV through calculation from three thermoluminescent curves obtained at 3 °C/min, 5 °C/min, and 8 °C/min heating rate, respectively. These trap levels were much higher than those in the Eu:SrAl₂O₄ sample prepared by a solid-state reaction process.⁶ That is why the sample of the present study gave comparative weak afterglow phenomena as shown in Figure 5.

The triboluminescent emission spectra of the Eu:SrAl₂O₄ peaked at the same wavelength as their PL spectra, that is, they also originated from the same mechanism — Eu²⁺ ion.⁶ Figure 7 shows a typical triboluminescent response curve of the SAO-E composites. The triboluminescent response was periodically modulated with a rotating speed of the rod. Each period denoted one peak and one valley. This oscillating change was also found in the other triboluminescence materials reported previously, such as ZnS:Mn,^{18,20} ZnAl₂O₄:Mn,²¹ MgGa₂O₄:Mn,²² etc., which may be caused by some nonuniformity of the test material, similar to the case of the bulk ceramics.²³ As shown in Figure 7, a tail was observed in the emission response curve after removing the load as a result of the long persistent behavior as discussed above (refer to Figure 5). Figure 8 shows the influence of the calcining temperature on the average triboluminescent intensity. The experimental data were well fitted using the first-order exponential decay. Therefore, the triboluminescent inten-

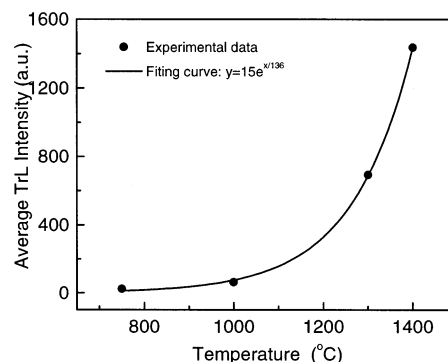


Figure 8. Influence of calcining temperature on triboluminescence.

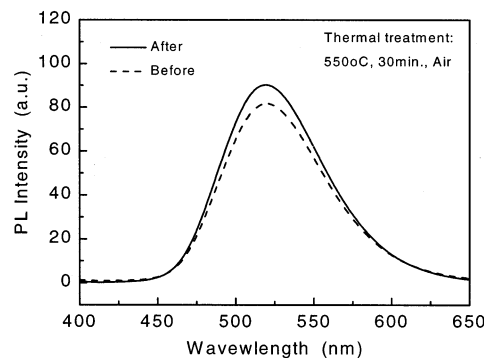


Figure 9. Thermal and oxidation-resistance in PL properties of Eu:SrAl₂O₄ powders.

sity exponentially increased with the calcining temperature, that is, the influence of the crystallinity of SAO-E particles on the triboluminescent intensity was significant, larger than that on the photoluminescence. This is similar to the results for other materials reported previously.^{20–22} A strong triboluminescent material should possess a pure phase of Eu:SrAl₂O₄.

The pure-phase Eu:SrAl₂O₄ particles also show a high stability in photoluminescent emission intensity after annealing at high temperature in air atmosphere due to its stable crystallized structure. Figure 9 shows the photoluminescent property of the Eu:SrAl₂O₄ particles before and after the heat-treatment in an air atmosphere at 600 °C for 30 min. The emission spectrum of the heat-treated Eu:SrAl₂O₄ particles did not show the red emission and the intensity degradation. On the other hand, SAO-E samples with a double phase of Sr₃Al₂O₆ and SrAl₂O₄ showed a remarkable decrease (drop down to 80%) after annealing in the same condition. This illustrates that the Eu²⁺ was not oxidized into the Eu³⁺ in the Eu:SrAl₂O₄ particles in the oxidation atmosphere up to 600 °C. This kind of phosphor particles without any thermal degradation will be extremely significant in practical application, such as the preparation of the luminescent coating, solidification of the phosphor/organic composites, and thermo-processing of the luminescent coating. We believe that this result has a great guiding significance for the other luminescent materials to overcome the thermal degradation.

Conclusions

A phase transformation from Sr₃Al₂O₆ to SrAl₂O₄ was found during the calcining process of the SAO-E particles. Accompanying this phase transformation, the light emission transition of SAO-E particles at low calcining temperature originated from both Eu²⁺ and Eu³⁺ ions, and the trivalent europium ions existed in the SrAl₂O₄ phase. The Eu³⁺ ions

gradually transformed into the Eu^{2+} ions with the increasing calcining temperature. A single monoclinic SrAl_2O_4 phase with a $P2_1$ space group can be obtained after calcining at 1400 °C for 2 h, where strong PL and triboluminescence from the Eu^{2+} ions are achieved. These pure $\text{Eu}:\text{SrAl}_2\text{O}_4$ powders are of high stability and showed no thermal degradation.

Acknowledgment. This work is partially supported by the Hayashi Memorial Foundation for Female Natural Scientists.

References and Notes

- (1) Matsuzawa, T.; Aoki, Y.; Takeuchi, N.; Murayama, Y. *J. Electrochem. Soc.* **1996**, *143* (8), 2670–2673.
- (2) Laud, K. R.; Gibbons, E. F.; Tien, T. Y.; Stadler, H. L. *J. Electrochem. Soc.* **1971**, *118* (6), 918–923.
- (3) Katsumata, T.; Sasajima, K.; Nabae, T.; Komuro, T.; Matsuzawa, T. *J. Am. Ceram. Soc.* **1998**, *81* (2), 413–416.
- (4) Tyner, C. E.; Drickamer, H. G. *J. Chem. Phys.* **1977**, *67* (9), 4116–4123.
- (5) Katsumata, T.; Nabae, T.; Sasajima, K.; Matsuzawa, T. *J. Cryst. Growth* **1998**, *183* (3), 361–365.
- (6) Xu, C. N.; Watanabe, T.; Akiyama, M.; Zheng, X. G. *Appl. Phys. Lett.* **1999**, *74* (17), 2414–2416.
- (7) Xu, C. N.; Liu, Y.; Akiyama, M.; Nonaka, K.; Zheng, X. G. *Optical Diagnostics for Fluids, Solids, and Combustion (Proceedings of SPIE)*, 4448, 2001; pp 398–407.
- (8) Xu, C. N. *Encyclopedia of Smart Materials*; Schwartz, M., Ed.; Wiley: New York, 2002; pp 190–201.
- (9) Xu, C. N.; Zheng, X. G.; Akiyama, M.; Nonaka, K.; Watanabe, T. *Appl. Phys. Lett.* **2000**, *76* (10), 179–181.
- (10) Ito, S.; Banno, S.; Suzuki, K.; Inagaki, M. *Yogyo-Kyokai-shi* **1979**, *87* (7), 344–349.
- (11) Murayama, G., etc. Japanese Patent H7-11250, 1995.
- (12) Tang, Z. L.; Zhang, F.; Zhang, Z. T.; Huang, C. Y.; Lin, Y. H. *J. Eur. Ceram. Soc.* **2000**, *20* (12), 2192–2132.
- (13) Song, Y. K.; Choi, S. K.; Moon, H. S.; Kim, T. W.; Mho, S. I.; Park, H. L. *Mater. Res. Bull.* **1997**, *32* (3), 337–341.
- (14) Vij, D. R. *Luminescence of Solids*; Plenum Press: New York, 1998; pp 122–123.
- (15) Jagannathan, R.; Kutty, T. R. N.; Kottaisamy, M.; Jeyagopal, P. *Jpn. J. Appl. Phys.* **1994**, *33*, 6207–6212.
- (16) Kamada, M.; Murakami, J.; Ohno, N. *J. Lumin.* **2000**, *87*–89, 1042–1044.
- (17) Jia, W.; Yuan, H.; Lu, L.; Liu, H.; Yen, W. M. *J. Lumin.* **1998**, *76&77*, 424–428.
- (18) Xu, C. N.; Zheng, X. G.; Akiyama, M.; Nonaka, K.; Watanabe, T. *Appl. Phys. Lett.* **1999**, *74* (9), 1236–1238.
- (19) Katsumata, T.; Nabae, T.; Sasajima, K.; Komuro, S.; Morikawa, T. *J. Electrochem. Soc.* **1997**, *144* (9), L243–245.
- (20) Xu, C. N.; Zheng, X. G.; Watanabe, T.; Akiyama, M.; Usui, I. *Thin Solid Films* **1999**, *352*, 273–277.
- (21) Matsui, H.; Xu, C. N.; Tateyama, H. *Appl. Phys. Lett.* **2001**, *78* (8), 1068–1070.
- (22) Matsui, H.; Xu, C. N.; Akiyama, M.; Watanabe, T. *Jpn. J. Appl. Phys.* **2000**, *39* (12), 6582–6586.
- (23) Nakayama, K. *Wear* **1996**, *194*, 185–189.